Electron-impact excitation of xenon at incident energies between 15 and 80 eV

D. Filipović,* B. Marinković, V. Pejčev, and L. Vušković
Institute of Physics, P.O. Box 57, 11001 Beograd, Yugoslavia
(Received 14 January 1987)

Normalized, absolute differential cross sections (DCS's) have been measured for the 20 lowest electronic states of xenon. Incident electron energies were 15, 20, 30, and 80 eV and the scattering angles ranged from 5° to 150°. The energy resolution was 40 meV. Absolute elastic DCS's have been obtained by normalizing the relative values to the recently published absolute elastic DCS's by Register *et al.* [J. Phys. B **19**, 1685 (1986)]. Elastic-to-inelastic intensity ratios, at different incident energies for the $6s[\frac{3}{2}]_1$ state were determined. These ratios were utilized as secondary standards to establish the absolute scale for the other inelastic processes in accordance with intensity ratios of lines in energy-loss spectra. The absolute inelastic DCS's were extrapolated to 0° and 180° and integrated to yield the integral cross sections (ICS's). A comparison of the present DCS's with the only available measurements at 20 eV impact energy shows satisfactory agreement in shape but considerable difference in absolute value.

I. INTRODUCTION

The investigation of xenon electron-impact excitation is of interest for completing a systematic survey of electron-noble-gas-atoms collision processes. Xenon has the largest atomic number of all the stable noble gases. Therefore, effects dependent on the size of a target atom, such as alignment and orientation of the atom after collisional excitation,[1] are best observed by studying this atom. Angular distributions associated with the various excitations range from sharp forward peaking to nearly isotropic, indicating the contribution of long-range coulombic and short-range exchange interactions.[2]

From a practical point of view, the absolute values of inelastic differential cross sections (DCS's) for the xenon atom are of interest for both laser and plasma physics,[3] calculation of electroluminescence intensity in xenon gas, proportional scintillation counters,[4] etc.

There are only a few quantitative experimental results of electron-impact excitation of specific electronic states in xenon. In fact, the normalized inelastic DCS's are given only in the article by Williams *et al.*[5] Recently, Nishimura *et al.*[6] presented some preliminary inelastic DCS data in the 10° to 125° angular range. Korotkov[7] has measured absolute integral cross-section (ICS) values for the two lowest metastable states of xenon.

An independent-particle model, including a distorted generalized oscillator strength method, has been applied for calculation of the total excitation cross sections.[8]

In Sec. II, we present a brief description of the apparatus as well as the experimental procedure. Results of the inelastic DCS's and ICS's with error estimation for both of them are presented in Sec. III. In Sec. IV, our results, as well as the systematic error in the results of Williams *et al.*[5] are discussed.

II. APPARATUS AND EXPERIMENTAL PROCEDURE

The electron spectrometer used in these measurements has already been described.[9] A collimated monoenergetic electron beam, produced by the monochromator (hairpin cathode, system of cylindrical electrostatic lenses and hemispherical electrostatic energy selector), was crossed with an atomic xenon beam generated by a Pt-Ir tube. The scattered electrons were analyzed by the rotatable (from $-30°$ to 150°) analyzer system. The analyzer was designed similarly to the monochromator. It consists of a system of cylindrical electrostatic lenses, a hemispherical electrostatic energy selector, and an electron multiplier. All of the electrodes were made of oxygen-free high-conductivity (OFHC) gold-plated copper, while the hemispheres and apertures were made of molybdenum.

Both the monochromator and analyzer were baked and differentially pumped with respect to the main vacuum chamber. The pressure in the chamber without target gas was 1×10^{-5} Pa, and the background pressure under normal operating conditions was 1×10^{-3} Pa. The density of the atomic beam in the interaction region was kept low enough so that the double scattering of the electron was negligible. The double μ-metal shield reduced the residual magnetic field to less than 0.1 μT. The energy scale was not calibrated in this experiment, and might have been in error by about 0.5–1.0 eV due to contact potentials.

The spectrometer works in the energy-loss mode, which means that for a given incident energy E_0, and for a given position of the analyzer (i.e., fixed scattering angle), the addition of energy to the inelastically scattered electrons is achieved by sweeping the analyzer potential.

If that addition is equal to the energy loss of incident electrons due to the excitation of target atoms to a particular electronic state, a line in the energy-loss spectrum will appear.

Electron lenses are always adjusted in such a way as to give the best possible energy resolution in order to resolve the lines in energy-loss spectra. The optimization does not correspond to the optimal count rate, but only to the increase of energy resolution. The optimal conditions correspond also to a minimal change of the intensity ratios of lines when the focusing changes. Since elastic and reference inelastic [state $6s[\frac{3}{2}]_1$) peaks are 8.4 eV apart, we found it best to first focus the intermediate region (4.2 eV energy loss) by using the background signal from the incident electron beam at a small scattering angle. Rather than transmission of the analyzer, we measured the "relative transmission," defined as the ratio of the intensities of a given peak when another one is focused and when it is focused itself. The same relative transmission values were obtained for the reference inelastic peak with respect to elastic peak, as well as for the elastic peak with respect to the reference inelastic peak.

To obtain the energy-loss spectra, the optics were always focused at the reference inelastic peak (8.4 eV energy loss). In a separate experiment, we optimized the optics in a way such that the transmissions for that peak and the peak containing the $5d[\frac{3}{2}]_1$ state (10.4 eV energy loss) were the same. The energy-loss spectra obtained in these experimental conditions were used for inelastic-to-reference inelastic intensity ratios needed for the determination of the inelastic DOS absolute scale.

The angular resolution as an angle at which the intensity of electron beam falls to half maximum was not determined experimentally. Since the atomic beam was formed by a 2.5-cm-long, 0.05-cm-diam. tube with back pressure of about 1 Torr, we believed that the interaction region was determined by the solid angle of the detector. Taking into account the geometry of the apparatus, we estimated its angular resolution of the experiment to be 1° to 2°.

An excellent agreement in shape between our relative elastic DCS (Ref. 10) and the absolute elastic DCS obtained by Register *et al.*[11] was the reason for the normalization of our results to those of Register *et al.* The xenon beam in that work was generated by a capillary array and further collimated by a skimmer (special arrangement for low angular resolution). This agreement with our present data confirmed our estimation of an angular resolution.

III. RESULTS

A. Elastic DCS's as a base for calibration of the reference inelastic (state $6s[\frac{3}{2}]_1$) cross sections

We have measured angular distributions for elastic electron-xenon atom scattering at 15, 20, 30, 50, 63, and 80 eV impact energies in the angular range from 15° to 150°.[10] As in other experiments of this kind, the real zero scattering angle has been determined from the symmetry of the scattering intensity in the $-30°$ to $-10°$ and $+30°$ to $+10°$ angular regions.

For each impact energy, the arithmetical mean value of more than three angular distributions, mutually normalized with respect to a relative value of a local maximum, was calculated. The effective path length correlation factors[12] were determined for the large-aspect-ratio tube ($\gamma=0.02$) and a DCS which decreases approximatively by three orders of magnitude from 0° to 90° scattering angle. The values given in Table I were obtained by extrapolating earlier results[12] to the 13 Pa (about 0.10 Torr) tube back pressure.

Finally, the absolute elastic DCS's were obtained by normalization with respect to the results of Register *et al.*[11] to the best agreement in shape. The agreement with results of Wagenaar *et al.*[13] for small angle (0° to 10°) elastic scattering of electrons by xenon atoms is proof of the validity of the results presented here (Fig. 1).

B. Angular distributions of inelastically scattered electrons

There are two ways of measuring angular distributions of inelastically scattered electrons on target-gas atoms: (a) by direct angular intensity distribution measurements of given features, and (b) by analysis of energy-loss spectra. Both of them were used in this work.

The first way is similar to the method used for elastic scattering. For a given incident energy and for a fixed energy loss, the scattering angle changes as a consequence of rotation of the analyzer. On the other hand, from the energy-loss spectra, angular distributions of the other inelastic features can be determined with respect to the known reference one.

A typical energy-loss spectrum for 20 eV impact energy and 100° scattering angle is shown in Fig. 2. The designation of spectral lines in this figure corresponds to that in Table II and is based on Moore's tables.[14]

TABLE I. Effective-path-length correction factor F.

F	θ (deg)	θ (deg)
0.83		15
0.84		20
0.86	155	25
0.87	150	30
0.89	145	35
0.91	140	40
0.93	135	45
0.94	130	50
0.95	125	55
0.96	120	60
0.97	115	65
0.98	110	70
0.99	105	75
0.99	100	80
1.0	95	85
1.0		90

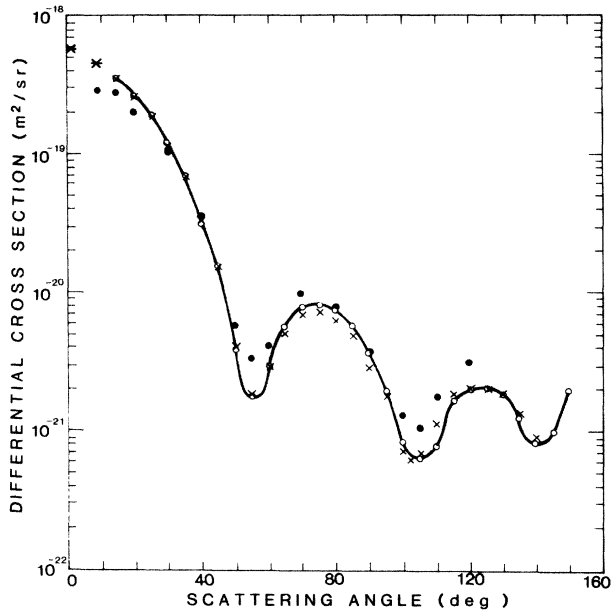

FIG. 1. Differential cross sections for elastic scattering of electrons by xenon atoms at 20 eV impact energy: ×, Register *et al.* (Ref. 11); ●, Nishimura *et al.* (Ref. 6); *, Wagenaar *et al.* (Ref. 13); and -○-, present results.

For each inelastic feature an angular distribution was calculated as the arithmetical mean value of three or more directly obtained curves matched with respect to a local maximum. Due to approximately equal statistical weights, the simple arithmetical mean value of the angular distributions was calculated from direct and energy-loss spectra measurements.

The same correction factors for effective path length used for elastic scattering were also used for inelastic features, except for the very strongly forward-peaking and nearly isotropic distributions.

Angular distributions were measured in the range of 5° to 150°. The lower limit in the angular range was determined by a signal-to-noise ratio lower than 100 due to the interferences of the incident electron beam. The upper limit was set by the finite monochromator and analyzer dimensions.

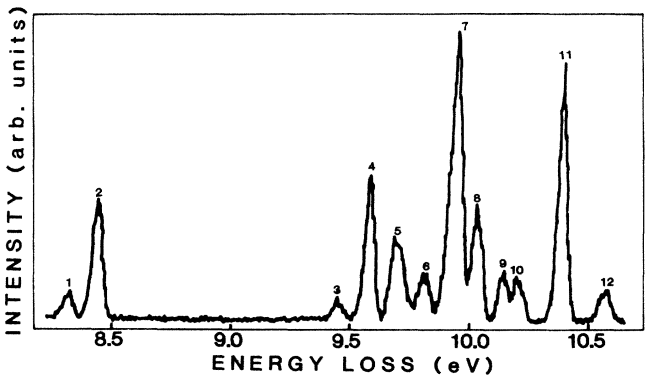

FIG. 2. Energy-loss spectrum of xenon at 20 eV impact energy at 100° scattering angle.

C. Differential cross sections

The measured (as explained in Sec. II) elastic-to-inelastic ($6s[\frac{3}{2}]_1$) intensity ratios are presented in Table III. The absolute DCS values for the $6s[\frac{3}{2}]_1$ state were obtained by using our absolute normalized elastic DCS and elastic-to-inelastic intensity ratios from Table III. These values are presented in Fig. 3 for 15, 20, 30, and 80 eV impact energies and in the angular range from 0° to 150°, with smooth curves drawn through the circles.

The absolute inelastic DCS values were determined for the 20 lowest electronic states of xenon. Some of them (seven) are resolved, while others are composite intensities unresolved in this experiment. Thus, DCS's for 12 features (see Fig. 2) are presented here. Seven of them (features 1, 2, 3, 8, 9, 10, and 11) are individual, four (features 4, 5, 6, and 12) are the overlap of two, and one (feature 7) is the overlap of five states.

The absolute inelastic DCS values are presented in Tables IV–VII. For 80 eV impact energy only the

TABLE II. Designation of the states of xenon and their energies.

Feature No.	State designation	Energy (eV)
Ground	$5p^6$	0.000
1	$6s[\frac{3}{2}]_2$	8.315
2	$6s[\frac{3}{2}]_1$	8.437
3	$6s'[\frac{1}{2}]_0$	9.447
4	$6s'[\frac{1}{2}]_1$	9.570
	$6p[\frac{1}{2}]_1$	9.580
5	$6p[\frac{5}{2}]_2$	9.686
	$6p[\frac{5}{2}]_3$	9.721
6	$6p[\frac{3}{2}]_1$	9.789
	$6p[\frac{3}{2}]_2$	9.821
7	$5d[\frac{1}{2}]_0$	9.891
	$5d[\frac{1}{2}]_1$	9.917
	$6p[\frac{1}{2}]_0$	9.934
	$5d[\frac{7}{2}]_4$	9.943
	$5d[\frac{3}{2}]_2$	9.959
8	$5d[\frac{7}{2}]_3$	10.039
9	$5d[\frac{5}{2}]_2$	10.158
10	$5d[\frac{5}{2}]_3$	10.220
11	$5d[\frac{3}{2}]_1$	10.401
12	$7s[\frac{3}{2}]_2$	10.562
	$7s[\frac{3}{2}]_1$	10.593

TABLE III. Elastic-to-inelastic (state $6s[\frac{3}{2}]_1$) intensity ratios.

I_{el}/I_{inel}	θ (deg)	E_0 (eV)
100	40	15
132	30	20
33	20	30
40	20	80

resolved features 2 and 11 were measured in the full angular range, due to very low intensities of other features at higher scattering angles. Besides the s state (Fig. 3), DCS's for the composite p states (Figs. 4 and 5) and individual d states (Figs. 6–8) are shown graphically by solid curves drawn through circles.

D. Integral cross sections

On the basis of absolute DCS values (Sec. III C), after extrapolation to 0° and 180° scattering angles, integral cross sections for particular features were obtained by numerical integration. Extrapolation to 0° was performed by experience with the other noble gases (argon[15] and krypton[16]), by continuing the slope of the curves at the lowest measured angles. The extrapolation procedure to 180° is less important due to the small contribution to the DCS at these angles to the integral cross section. For instance, the relative difference is within 5% for extrapolation with constant value (DCS value at 150°) and if this contribution to the integral cross section is neglected for the $6s[\frac{3}{2}]_1$ state at 15 eV impact energy. Because there are no experimental or theoretical results for large-angle inelastic scattering of slow electrons by xenon atoms, a constant value of DCS was used above 150° (equal to the value at 150°). A summary of the absolute integral cross-section values is given in Table VIII.

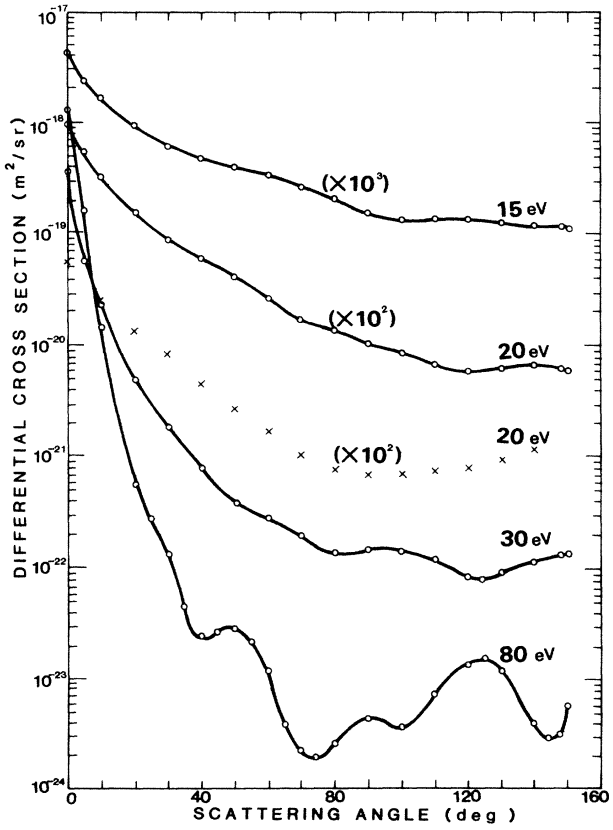

FIG. 3. Differential cross sections for the $6s[\frac{3}{2}]_1$ state (feature 2) at different impact energies: ×, Williams *et al.* (Ref. 5); -○-, present results.

E. Error estimation

We estimated the maximum error for each investigated feature. Estimations were performed under the following conditions.

Statistical errors in these inelastic scattering experiments were always within 10% in individual measurements. There are a few cases with larger statistical errors due to very low signal intensity. Such results are shown in the figures with statistical error bars of the data points.

A contribution to the systematic error for the relative values of inelastic DCS's due to the uncertainty of the energy is estimated as 5%, that due to the uncertainty of the angular scale as 3%, and that due to the applied geometrical correction factor as 5%. Rough deconvolution overlapping of the features 9 and 10 contributes an additional error of less than 5% to the DCS's. Thus, the total error (as the square root of the sum of squares) for the relative DCS values is less than 13%, with the exception of features 9 and 10, for which the error is less than 14%.

A very good agreement in the shape of our elastic DCS curves with respect to the results obtained by Register *et al.*[11] indicates that the normalization error for the inelastic DCS is within 5%. Including the error of the reference elastic DCS, the total error of our elastic DCS was 8% for $E_0=15$ and 20 eV, and 11% for $E_0=30$ and 80 eV.

An experimental determination of elastic-to-reference inelastic intensity ratios contributes 15% to the error for the absolute DCS of the reference inelastic feature at 15 eV impact energy and 10% for the other impact energies.

A determination of inelastic-to-reference inelastic intensity ratios contributes less than 5% to the error of the absolute DCS of measured inelastic features at each numbered energy.

On the basis of the estimated errors mentioned above, "levels of error" were found. For the reference $6s[\frac{3}{2}]_1$ state the estimated levels of error were 22%, 19%, and 21% at 15, 20, and both 30 and 80 eV impact energies, respectively. For the other inelastic features the estimated levels of error were 20% at 20 eV and 25% at the other impact energies.

TABLE IV. Inelastic differential cross sections σ (Xe) at $E_0=15$ eV impact energy in units of 10^{-23} m^2/sr. For 0° scattering angle DCS values are obtained by extrapolation.

θ (deg) \ Line	1	2	3	4	5	6	7	8	9	10	11	12
0	34.9	412	5.97	136	60.7	21.2	89.6	11.5	3.78	1.59	30.9	15.9
5	30.9	224	5.48	69.7	39.8	15.9	70.2	11.0	3.86	1.89	24.4	7.12
10	26.9	159	5.83	50.8	32.7	15.6	49.8	11.2	4.78	2.17	20.9	4.33
20	19.7	90.6	7.83	33.8	25.7	11.7	61.8	10.9	4.98	2.30	23.5	4.40
30	12.3	59.5	5.39	31.0	22.9	9.53	68.2	10.9	6.13	2.48	26.9	3.64
40	9.07	46.5	6.13	33.5	22.5	8.79	70.3	11.9	7.91	3.78	33.1	6.93
50	6.79	38.8	4.78	37.2	20.0	8.23	63.6	12.8	9.13	4.39	38.8	7.03
60	5.24	32.2	4.08	36.6	17.4	7.50	58.2	13.8	9.81	4.41	35.0	6.11
70	4.45	24.6	3.51	32.0	13.0	6.34	56.9	14.0	9.59	4.18	30.0	5.36
80	5.00	20.0	3.47	26.0	10.2	5.63	62.0	15.0	10.1	4.20	28.2	5.19
90	3.85	15.2	3.17	18.6	7.24	4.77	58.1	14.1	8.96	3.93	23.0	4.43
100	4.47	13.1	2.89	17.1	5.98	4.60	57.6	13.9	9.07	4.30	18.8	4.20
110	4.88	13.5	3.17	19.9	6.77	5.28	58.5	13.9	9.83	4.47	15.1	4.50
120	4.32	13.3	3.27	20.8	9.34	5.61	52.6	12.6	9.96	4.13	11.8	4.27
130	6.99	12.5	3.22	19.1	12.8	5.71	45.9	10.8	8.62	3.32	11.1	4.06
140	7.16	11.7	3.22	17.8	16.4	5.87	39.0	8.73	7.05	2.59	12.2	3.84
148	8.36	11.2	3.31	18.6	20.4	6.07	35.6	7.06	5.70	2.03	18.0	3.45
150	8.54	11.0	3.29	18.6	21.3	6.07	34.8	6.68	5.32	1.93	18.6	3.32

Integral cross-section values included additional errors due to the extrapolation of the DCS to 0° and 180° scattering angles and due to a finite number of steps in numerical integration. The estimated error is 15% due to extrapolation and 5% due to numerical integration, except for $E_0=80$ eV, for which the error is 25% and 10%, respectively, because of the remarkable forward peaking. Thus, the estimated levels of error for integral cross sections are 30%, except for $E_0=80$ eV, with the estimated level of 38%.

IV. DISCUSSION AND CONCLUSION

In the ground state the xenon atom has an electron configuration of

$$1s^2 2s^2 2p^6 3s^2 3p^6 3d^{10} 4s^2 4p^6 4d^{10} 5s^2 5p^6 .$$

Excitation to the lowest electronic states investigated in this work goes via transition of the $5p$ electron to $6s$ or some of the nearest higher free orbits. In this way an excited atom can be considered as the Xe^+ ion core plus

TABLE V. Inelastic differential cross sections σ (Xe) at $E_0=20$ eV impact energy in units of 10^{-23} m^2/sr. For 0° scattering angle DCS values are obtained by extrapolation.

θ (deg) \ Line	1	2	3	4	5	6	7	8	9	10	11	12
0	23.0	978	11.5	610	196	78.8	357	23.0	3.68	1.55	242	132
5	15.4	549	7.19	255	85.6	43.9	192	11.4	3.19	1.73	165	59.2
10	12.1	319	4.83	140	47.9	26.1	125	7.01	2.55	2.16	89.7	31.5
20	9.82	140	4.21	67.4	28.3	13.3	77.2	7.29	2.53	2.60	67.6	13.8
30	7.62	84.7	4.06	54.5	21.2	10.3	65.6	10.2	4.31	3.76	69.4	11.0
40	6.34	59.8	4.07	44.9	17.0	9.27	61.0	10.8	7.78	4.30	64.7	11.4
50	5.02	41.8	3.59	33.8	13.6	8.56	55.3	11.8	8.77	5.02	51.0	10.0
60	4.52	26.6	2.66	23.9	9.43	6.37	44.2	10.9	7.30	4.26	35.7	7.44
70	3.13	16.5	1.83	18.8	6.25	4.00	34.4	8.88	5.51	3.62	23.4	4.94
80	2.17	12.5	1.63	12.8	5.02	2.47	31.9	8.52	4.96	3.70	17.8	3.64
90	1.63	10.2	1.55	9.79	4.49	2.55	28.3	7.13	4.49	3.82	14.3	2.35
100	1.65	8.43	1.54	11.0	5.76	2.86	24.5	7.34	4.34	4.13	16.0	2.02
110	1.85	6.87	1.77	12.0	6.29	3.70	34.3	9.62	3.95	3.98	20.8	3.43
120	2.58	5.73	.989	8.88	6.02	2.98	39.7	7.21	3.44	2.75	14.5	3.44
130	2.86	6.37	.905	5.83	4.56	2.16	26.7	5.10	2.55	2.16	9.81	2.74
140	2.80	6.98	1.48	6.84	9.92	4.05	29.7	5.17	2.86	2.09	14.6	2.97
148	2.93	6.38	2.30	12.4	11.7	5.14	28.3	5.31	3.06	2.13	25.5	4.61
150	2.83	5.89	2.42	13.6	11.3	5.19	26.5	5.06	3.06	2.00	28.3	4.83

TABLE VI. Inelastic differential cross sections σ (Xe) at $E_0 = 30$ eV impact energy in units of 10^{-23} m^2/sr. For 0° scattering angle DCS values are obtained by extrapolation.

θ (deg) \ Line	1	2	3	4	5	6	7	8	9	10	11	12
0	47.3	35500	64.2	7100	744	270	1010	14.2	5.75	25.7	5540	1150
5	35.8	5540	48.3	2570	487	176	304	19.3	6.15	29.1	2910	548
10	30.8	2220	32.2	1180	317	148	101	21.2	6.55	30.7	1500	312
20	16.6	465	10.1	299	120	46.8	99.4	31.2	8.93	35.4	393	96.0
30	11.6	168	5.09	105	33.3	13.1	54.9	21.5	5.13	20.9	178	42.6
40	7.44	75.1	1.74	46.5	25.1	6.38	40.4	11.3	3.72	12.3	98.1	17.4
50	2.56	35.8	1.23	24.1	7.30	5.29	48.8	7.64	3.77	5.77	39.3	10.5
60	1.61	26.1	1.12	28.8	8.39	4.50	71.0	9.67	3.53	5.78	29.1	9.33
70	0.588	17.9	0.539	15.4	5.29	1.87	43.9	7.64	1.56	4.02	16.4	6.76
80	1.17	12.0	0.292	9.67	3.71	2.63	30.6	6.83	2.25	5.94	16.9	3.52
90	0.524	12.8	0.0525	8.79	2.83	2.41	22.6	4.19	1.78	2.10	9.26	4.19
100	0.440	12.6	0.176	10.8	2.98	1.32	26.5	3.69	1.14	2.20	8.25	3.52
110	0.879	11.0	0.293	7.98	3.90	3.03	35.8	3.03	1.56	1.66	13.5	2.35
120	0.410	8.25	0.245	6.76	2.54	1.47	32.6	4.10	1.72	1.72	14.7	2.05
130	0.423	9.20	0.423	6.67	3.60	2.64	26.7	5.94	1.37	3.07	14.0	2.75
140	0.960	10.7	0.642	12.2	3.84	3.74	21.8	4.50	3.84	3.74	18.2	2.79
148	0.933	12.7	0.511	14.6	5.71	4.68	32.1	3.58	1.96	2.30	18.9	2.81
150	0.933	12.8	0.500	14.7	5.95	4.73	35.8	3.45	1.69	2.28	18.8	2.81

TABLE VII. Inelastic differential cross sections σ (Xe) at $E_0 = 80$ eV impact energy in units of 10^{-23} m^2/sr. Quantities shown in parentheses are obtained by extrapolation.

θ (deg) \ Line	2	11
0	(177 000)	(22 000)
5	15 700	(7700)
10	1380	1610
20	55.5	85.9
25	25.6	28.6
30	12.1	13.2
35	4.32	7.29
40	2.36	3.81
45	2.48	2.77
50	2.68	2.84
55	2.11	
60	1.12	1.25
65	0.374	
70	0.223	0.381
74	0.204	
80	0.242	0.530
90	0.429	0.536
100	0.353	0.577
110	0.714	0.995
120	1.26	1.59
125	1.41	1.71
130	1.16	1.46
140	0.402	6.29
144	0.296	9.34
148	0.322	15.8
150	0.576	(16.5)

excited e^- system. Since two different values of angular momentum of the ion core, $J_c = \frac{1}{2}$ or $\frac{3}{2}$ are possible, two classes of states, denoted by $s',p',d',f',\ldots$ and $s,p,d,f,\ldots$, of the excited electron do exist. For xenon the coupling schemes are different for different excited states, and the $J1$ coupling scheme recommended by Racah[17] is usually suggested.

The DCS curves for s states, generally speaking, are similar in shape to the elastic DCS curves, especially for large angles. Larger differences for lower angles (i.e., larger impact parameters) can be explained by the appearance of long-range coulombic forces of the excited atom. For higher impact energies the similarity is greater (see Fig. 3), because the incident electron crosses the field of the distorted target atom more rapidly.

The lines in the energy-loss spectra which correspond to transitions to p states were unresolved in this work, but DCS values for composite $6p$ states were given.

For $5d$ states DCS's are nearly isotropic, especially for lower energies, except for the $5d[\frac{3}{2}]_1$ state with slightly forward-peaked cures, especially for higher energies.

Integral cross sections for s and d states show satisfactory agreement in the general position of data points with respect to the integral cross-section curves for argon.[18]

There is only a very limited amount of quantitative results for electron impact excitation of electronic states in xenon. In the article by Williams *et al.*[5] inelastic DCS's are given for xenon at 20 eV impact energy and in the angular range up to 140°. Satisfactory agreement in shape exists between this curve and our DCS curve, but

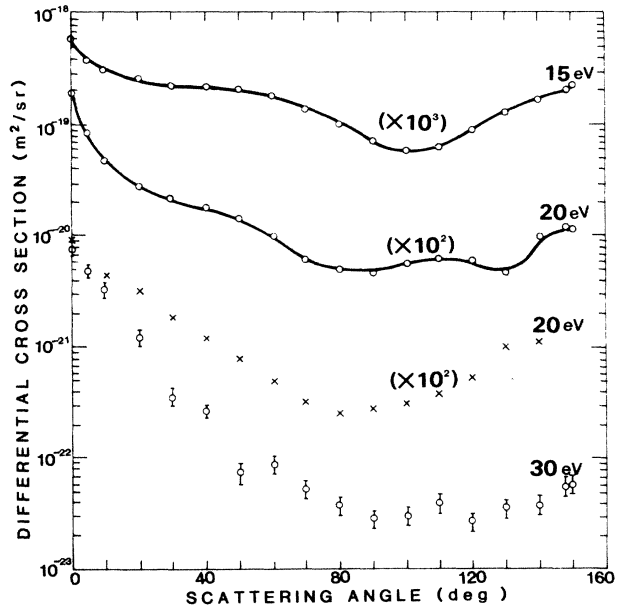

FIG. 4. Differential cross sections for the overlapped $6p[\frac{5}{2}]_2$ and $6p[\frac{5}{2}]_3$ states (feature 5) at different impact energies: ×, Williams *et al.* (Ref. 5); -○-, present results.

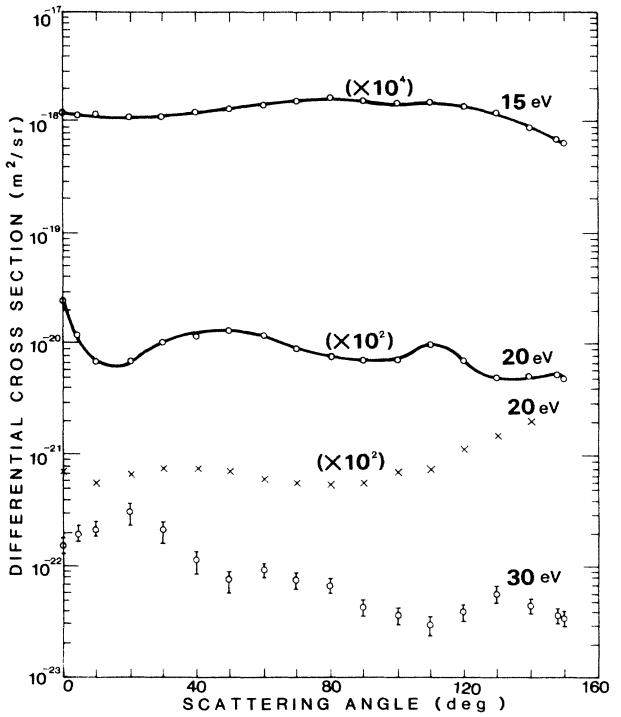

FIG. 6. Differential cross sections for the $5d[\frac{7}{2}]_3$ state (feature 8) at different impact energies: ×, Williams *et al.* (Ref. 5); -○-, present results.

the disagreement in the absolute values is significant. The normalization procedure in the work mentioned above was based on total electron-xenon cross-section values measured previously and presented by Massey and Burhop.[19] Those cross-section values were obtained by the Ramsauer technique[20] and they were systematically lower. Reduction in the measured absorption ap-

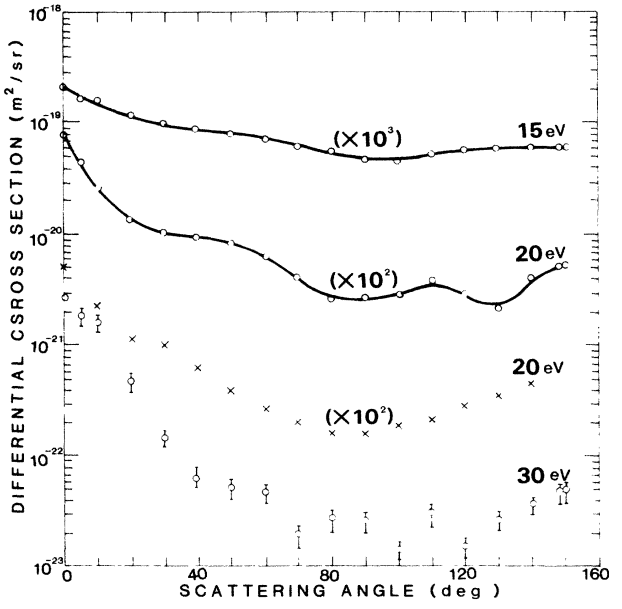

FIG. 5. Same as Fig. 4, but for the overlapped $6p[\frac{3}{2}]_1$ and $6p[\frac{3}{2}]_2$ states (feature 6).

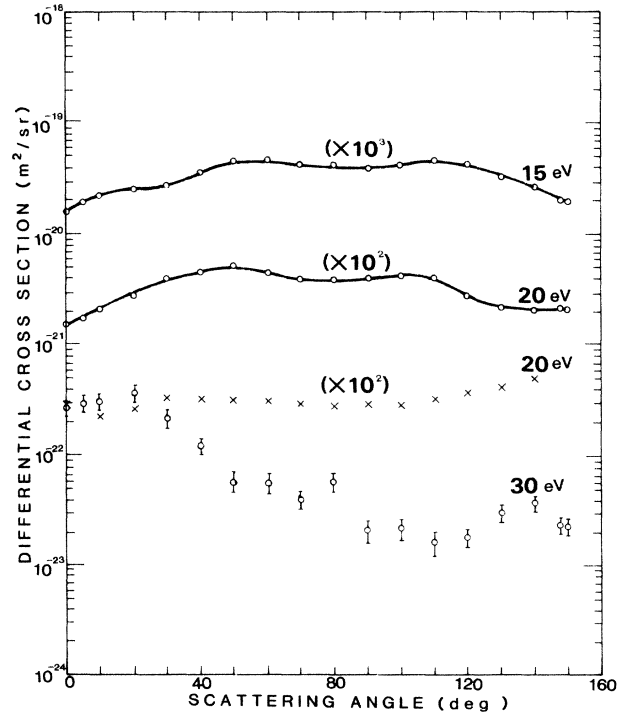

FIG. 7. Same as Fig. 6, but for the $5d[\frac{5}{2}]_3$ state (feature 10).

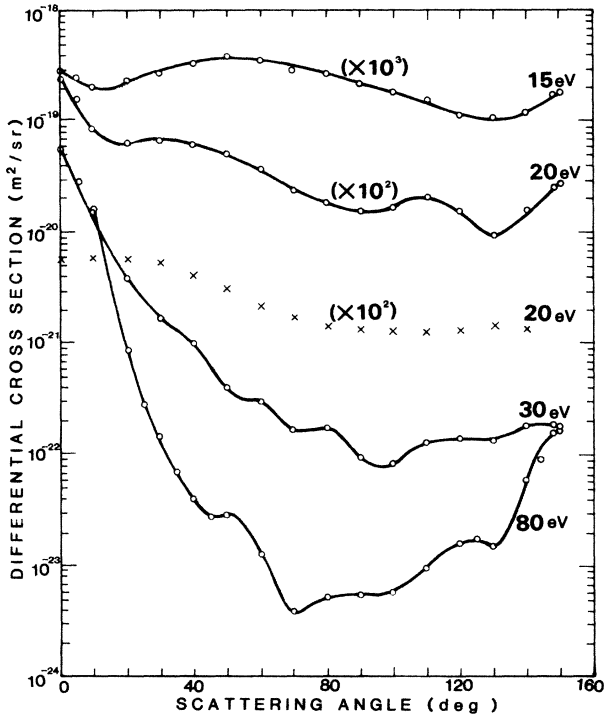

FIG. 8. Same as Fig. 6, but for the $5d[\frac{3}{2}]_1$ state (feature 11).

TABLE VIII. Integral cross sections for electron impact excitation of xenon in units of 10^{-23} m^2.

Feature	E_0 (eV) 15	20	30	80
1	85.9	44.6	34.6	
2	336	360	1400	1750
3	48.4	27.7	20.4	
4	321	276	684	
5	180	126	205	
6	83.4	66.7	95.0	
7	697	500	517	
8	155	102	94.3	
9	107	59.2	32.9	
10	46.2	43.4	76.6	
11	290	370	888	735
12	60.4	73.4	200	
Sum of the ICS's (present work)	2410	2050	4250	>2480
Sum of the ICS's by Williams *et al.* (Ref. 5)		223		
Recommended values for the total excitation cross section by Hayashi (Ref. 21)	2140	3730	3570	1660

pears due to difficulties in controlling the spatial extension of the electron beam in this type of apparatus. On the other hand, the elastic-to-inelastic intensity ratio obtained by Wiliams and co-workers is larger than that obtained in this work. These two differences cause disagreement of up to one order of magnitude (our DCS values are higher).

In the paper by Korotkov[7] ICS's for electron impact excitation of the $6s[\frac{3}{2}]_2$ and $6s'[\frac{3}{2}]_0$ states of xenon are given. His experimental technique includes an incident electron beam and collection of electrons from collision processes of xenon metastables with metal surfaces. His results at 28.9 eV impact energy are larger by about a factor of 1.5 for the $6s'[\frac{1}{2}]_0$, and by about a factor of 4 for the $6s[\frac{3}{2}]_2$ state than ours at 30 eV.

Using at atomic independent-particle model for the calculation of distorted generalized oscillator strengths, Ganas and Green[8] have obtained a total excitation cross section for unresolved $5p$-$6s$ transitions. The calculated values (in the energy range 15–80 eV) are lower by approximately a factor of 3 with respect to the results obtained here as a sum of integral cross sections for the lowest four clearly unresolved $6s$ states.

Sums of the individual ICS's measured in this work are shown in Table VIII. For comparison, the results by Williams *et al.*,[5] as well as Hayashi's[21] recommended values of total excitation cross sections, are included too.

Thus, on the basis of normalized elastic DCS values and separately measured elastic-to-inelastic intensity ratios, the absolute inelastic DCS values for the xenon atom were obtained in this work. An energy resolution of about 40 meV was sufficient to separate seven individual states, besides four unresolved (overlap of two) and one unresolved (overlap of seven) states.

The absolute inelastic DCS's and ICS's for 15, 30, and 80 eV impact energy are obtained for the first time and presented in this paper. New exact measurements as well as theoretical calculations about electron-xenon atom scattering processes can be expected.

ACKNOWLEDGMENTS

We would like to thank Professor Dr. Milan Kurepa and Dr. Iztok Čadež for many fruitful discussions. This work has been supported by the Republic Council of Scientific Research of the Socialist Republic of Serbia, Yugoslavia, and partly by the National Bureau of Standards (Grant No. JFP 598).

*Permanent address: Technical Faculty, Novi Sad University, 21000 Novi Sad, Yugoslavia.

[1]N. Andersen, J. W. Gallagher, and U. V. Hertel, in *Invited Papers of the Fourteenth International Conference on the Physics of Electronic and Atomic Collisions,* edited by M. J. Coggiola, D. L. Huestis, and R. P. Saxon (ICPEAC, Palo Alto, 1985), p. 57; and private communication.

[2]A. Kuppermann, J. K. Rice, and S. Trajmar, J. Phys. Chem.

72, 3894 (1968).

[3]M. Z. Novgorodov, *Investigation of Plasmas of Molecular Lasers,* edited by N. G. Basov (USSR Academy of Science, Moscow, 1974), Vol. 78, p. 105.

[4]T. H. V. T. Dias, A. D. Stauffer, and C. A. N. Conde, IEEE Trans. Nucl. Sci. **NS-30**, 389 (1983).

[5]W. Williams, S. Trajmar, and A. Kuppermann, J. Chem. Phys. **62**, 3031 (1975).

[6]H. Nishimura, A. Danjo, and T. Matsuda, *Abstracts of Contributed Papers of the Fourteenth International Conference on the Physics of Electronic and Atomic Collisions, Palo Alto, 1985,* edited by M. J. Coggiola, D. L. Huestis, and R. P. Saxon (ICPEAC, Palo Alto, 1985), p. 108.

[7]A. I. Korotkov, Abstracts of Proceedings of the Ninth All-Union Conference on the Physics of Electronic and Atomic Collisions, Riga, 1984 (in Russian), Part 2, p. 40.

[8]P. S. Ganas and A. E. S. Green, Phys. Rev. A **4**, 182 (1971).

[9]B. Marinković, Cz. Szmytkowski, V. Pejčev, D. Filipović, and L. Vušković, J. Phys. B **19**, 2365 (1986).

[10]B. Marinković, V. Pejčev, D. Filipović, and L. Vušković, in *Abstracts of Contributed Papers of the Thirteenth International Conference on the Physics of Electronic and Atomic Collisions, Berlin, 1983,* edited by J. Eichler, W. Fritsch, I. V. Hertel, N. Stolterfoht, and U. Wille (North-Holland, Amsterdam, 1983), p. 85.

[11]D. F. Register, L. Vušković, and S. Trajmar, J. Phys. B **19**, 1685 (1986).

[12]R. T. Brinkmann and S. Trajmar, J. Phys. E **14**, 245 (1981).

[13]R. W. Wagenaar, A. de Boer, J. van Tubergen, J. Los, and F. J. de Heer, J. Phys. B **19**, 3121 (1986).

[14]C. E. Moore, *Atomic Energy Levels,* Natl. Bur. Stand. (U.S.) Circ. No. 467 (U.S. GPO, Washington, D.C., 1958), Vols. I–III.

[15]D. Filipović, V. Pejčev, B. Marinković, and L. Vušković, in *Abstracts of Contributed Papers of the Eleventh Symposium on the Physics of Ionized Gases, Dubrovnik, 1982,* edited by G. Pichler (Institute of Physics of the University, Zagreb, 1982), p. 23.

[16]D. Filipović, S. Kazakov, B. Marinković, Cz. Szmytkowski, V. Pejčev, and L. Vušković, in *Abstracts of Contributed Papers of the Thirteenth Symposium on the Physics of Ionized Gases, Šibenik, 1986,* edited by M. V. Kureva (University of Belgrade, Belgrade, 1986), p. 3.

[17]G. Racah, Phys. Rev. **61**, 537(L) (1942).

[18]A. Chutjian and D. C. Cartwright, Phys. Rev. A **23**, 2178 (1981).

[19]H. S. W. Massey and E. H. S. Burhop, *Electronic and Ionic Impact Phenomena* (Clarendon, Oxford, 1969), Vol. I, p. 25.

[20]C. Ramsauer, Ann. Phys. **64**, 513 (1921); **66**, 546 (1921).

[21]M. Hayashi, J. Phys. D **16**, 581 (1983).